





# Assessing the Performance of NMF and GMM in the Soft Classification of Kidney Stones: Insights from FTIR Data

Aistis Raudys<sup>1</sup> , Aušra Šubonienė<sup>2</sup> , and Arūnas Želvys<sup>3,4</sup>

<sup>1</sup> Institute of Computer Science, Vilnius University,  
Didlaukio g. 47, 08303 Vilnius, Lithuania

[aistis.raudys@mif.vu.lt](mailto:aistis.raudys@mif.vu.lt)

<sup>2</sup> Institute of Data Science and Digital Technologies, Vilnius University,  
Akademijos g. 4, 08412 Vilnius, Lithuania

[ausra.suboniene@mif.vu.lt](mailto:ausra.suboniene@mif.vu.lt)

<sup>3</sup> Institute of Clinical Medicine, Faculty of Medicine, Clinic of Gastroenterology,  
Nephrourology and Surgery, Vilnius University, M. K. Čiurlionio g. 21/27,  
03101 Vilnius, Lithuania

[arunas.zelvys@santa.lt](mailto:arunas.zelvys@santa.lt)

<sup>4</sup> Center of Urology, Vilnius University Hospital Santaros Klinikos,  
Santariškiu g. 2, 08660 Vilnius, Lithuania

<https://mif.vu.lt/lt3/en/about/structure/institute-of-computer-science/> ,  
<https://mii.lt>

**Abstract.** In the management of kidney stones, identifying the stones' composition is crucial for determining appropriate treatment methods, as different compositions may require different treatment strategies. This study introduces a novel approach utilising Fourier Transform Infrared (FTIR) spectra data to determine kidney stones' composition. By using non-negative matrix factorisation (NMF) for dimensionality reduction and Gaussian mixture model (GMM) for Bayesian soft classification, this method aims to offer a faster and non-destructive alternative to other traditional methods, such as wet chemistry. Initial findings indicate that this approach can effectively analyse kidney stones' composition, showing promise even in cases with limited sample sizes. The application of NMF and GMM to FTIR data could significantly improve the efficiency and accuracy of kidney stones' composition analysis, potentially leading to more effective treatment options.

**Keywords:** Kidney stones · FTIR spectroscopy · Gaussian mixture model

## 1 Introduction

The analysis of kidney stones is a critical component in the management and treatment of urolithiasis, offering insights into the etiology and optimal treatment pathways for patients. Despite advancements in analytical techniques,

© The Author(s), under exclusive license to Springer Nature Switzerland AG 2025

A. Lopata et al. (Eds.): ICIST 2024, CCIS 2401, pp. 48–60, 2025.

[https://doi.org/10.1007/978-3-031-84263-4\\_5](https://doi.org/10.1007/978-3-031-84263-4_5)

challenges still exist to accurately identify the composition of kidney stones, especially when considering the variety of kidney stones' types, including rare ones like cyanoacrylate and pyrophosphate stones. Techniques such as Fourier Transform Infrared (FTIR) spectroscopy, combined with neural networks, have shown promise in leveraging extensive datasets to enhance identification accuracy. However, the precision of these methods, especially involving small sample sizes, remains a subject of ongoing evaluation. This complexity is compounded by the necessity of differentiating between primary and secondary stone components, where traditional methods sometimes fall short. As some kidney stones' types are exceedingly rare, there is a pressing need for innovative approaches that can accurately identify stones' composition across a spectrum of sample sizes, ensuring tailored and effective treatment plans for patients.

### 1.1 Variations in the Treatment and Management of Various Kidney Stones' Compositions

Treatment strategies for kidney stones vary notably depending on the stones' type and are not only different, but also sometimes conflicting. For calcium oxalate stones, the most prevalent type of kidney stones [1,2], management focuses on dietary changes and increased fluid intake to prevent stone formation and facilitate passage. Specific recommendations include reducing oxalate-rich foods and ensuring adequate dietary calcium [3]. Struvite stones, tied to urinary infections, require antibiotics for treating the infection and surgical removal of stones to avert recurrence [4]. Uric acid stone treatment emphasizes urine alkalization with potassium citrate and diet adjustments to reduce uric acid levels, aiming at dissolving the stones chemically [5]. Cystine stones, arising from a genetic condition that increases cystine in urine, call for extensive urine alkalization and chelating agents to boost solubility [6]. These differentiated approaches underline the critical need for a deep understanding of each stone's etiological and chemical characteristics to guide targeted treatments that address the specific causes and risks of recurrence. This emphasizes the role of tailored dietary and pharmacological interventions alongside surgical options, based on the unique properties of each stone type.

### 1.2 Fourier Transform Infrared (FTIR) Spectroscopy

Fourier Transform Infrared (FTIR) spectroscopy is an analytical technique used to obtain an infrared spectrum of absorption or emission of a solid, liquid, or gas. Measurements taken with FTIR spectroscopy are straightforward, quick, accurate, and non-destructive, making it an efficient method for analyzing the molecular composition of samples [12]. FTIR spectroscopy involves the exposure of a sample (a kidney stone that was removed from the patient) to a broad spectrum of infrared light, allowing for the measurement of the sample's absorbance and transmission of light across the infrared region, typically between 4000 to 400  $\text{cm}^{-1}$ . Molecules within the sample absorb infrared radiation at frequencies

that correspond to their vibrational modes, leading to a unique spectral fingerprint. This absorption is due to the changes in the dipole moment of the molecule, making it possible to identify functional groups and, by extension, the molecular structure of the material that is being analysed. The Fourier Transform, a mathematical algorithm, is then applied to convert the raw data obtained from the interferogram into a spectrum that represents the intensity of absorption or transmission as a function of frequency or wavelength:

$$S(\nu) = \int_{-\infty}^{\infty} I(t) \cdot e^{-2\pi i \nu t} dt \quad (1)$$

where  $S(\nu)$  is the Fourier Transform of  $I(t)$ , representing the frequency domain spectrum,  $I(t)$  is the time-domain signal obtained from the FTIR measurement,  $\nu$  is the frequency variable, representing the number of cycles per unit time.

### 1.3 Utilizing FTIR Spectroscopy for the Analysis of Kidney Stones' Characteristics

Integrating the use of Fourier Transform Infrared (FTIR) spectroscopy into kidney stones' analysis has shown considerable promise, particularly in identifying rare stones' types like cyanoacrylate and pyrophosphate, as explored in [7]. The potential of FTIR spectroscopy for such specific detections highlights its significance in the broader context of urinary stone analysis. Additionally, the application of FTIR microscopy for chemical mapping, as detailed by [8], has been instrumental in depicting the chemical compound distribution within kidney stones, providing a granular view of their composition and structure.

In a notable study involving the analysis of 800 kidney stones' samples through FTIR, the variation in protein concentration relative to the stones' composition was documented [9]. This research found a pronounced variation in protein content across different stone types, with higher concentrations noted in stones that were a mix of calcium apatite and calcium oxalate dihydrate, among others. Conversely, the stones composed primarily of cystine, urate, and calcium oxalate monohydrate exhibited lower protein levels, with the patient's age being a factor in these differences. This finding underscores the utility of FTIR spectroscopy in not only identifying the stones' composition, but also in providing insights into the biochemical environment of stones' formation.

A study by [10] highlighted discrepancies when cross-validating FTIR results with those obtained from the chemical analysis and X-ray diffraction (XRD), suggesting areas for methodological improvement. The outcomes from chemical analysis (CA) were inconsistent with those obtained via FTIR spectroscopy in 56% of instances. Specifically, CA failed to identify the primary component of the stone in 16% of the cases and overlooked the secondary component in 40% of the instances. Moreover, the integration of FTIR spectroscopy with neural network analysis, leveraging a vast database of over a million kidney stones' spectra as demonstrated by [11], represents a significant leap forward in stones' composition identification.

Still, the extent of precision in these predictions, particularly with smaller sample sizes, remains somewhat uncertain. This concern is amplified considering that the most effective results reported in the literature have been achieved through the use of neural networks and extensive datasets comprising over one million kidney stones. Given that some types of kidney stones are exceedingly rare, alternative methods are necessary for the composition identification of kidney stones when dealing with limited sample quantities.

## 2 Methods

### 2.1 Non-negative Matrix Factorization (NMF)

Non-negative Matrix Factorization (NMF) is particularly useful in analyzing FTIR spectroscopy data, especially when investigating complex materials such as kidney stones. In the context of FTIR data, NMF decomposes a matrix  $V$  of spectral data into two matrices,  $W$  and  $H$ , where  $V$  represents the observed FTIR spectra,  $W$  represents the basis spectra (or the spectral signatures of the components), and  $H$  represents the abundance or concentration of these components across the samples. The key constraint, that all elements in  $V$ ,  $W$ , and  $H$  are non-negative, aligns well with the nature of FTIR data, where the intensity of absorption at different wavelengths cannot be negative.

The factorization can be represented by the formula:

$$V \approx WH, \quad (2)$$

where  $V$  is an  $n \times m$  matrix, where  $n$  is the number of different wavelengths measured across  $m$  samples.  $W$  is an  $n \times r$  matrix, where  $r$  represents the number of distinct components or materials that the algorithm identifies within the kidney stones, and each column in  $W$  represents the spectral signature of one component.  $H$  is an  $r \times m$  matrix, where each column corresponds to a sample's composition in terms of the  $r$  components.

The objective function, using the Frobenius norm, is defined as:

$$\min_{W, H} \|V - WH\|_F^2 \quad (3)$$

subject to  $W \geq 0$  and  $H \geq 0$ .

To find the best  $W$  and  $H$ , an iterative method is used to update matrices  $W$  and  $H$ . The multiplicative update rules for  $H$  and  $W$  are:

$$H_{au} \leftarrow H_{au} \frac{(W^T V)_{au}}{(W^T W H)_{au}}, \quad W_{ia} \leftarrow W_{ia} \frac{(V H^T)_{ia}}{(W H H^T)_{ia}} \quad (4)$$

To mitigate the potential for overfitting and to regularize the solution space, additional penalization terms are introduced into the objective function. These terms impose a constraint on the complexity of  $W$  and  $H$  by penalizing their Frobenius norms. Consequently, the revised objective function is formulated as:

$$\min_{W, H} \|V - WH\|_F^2 + \lambda_W \|W\|_F^2 + \lambda_H \|H\|_F^2 \quad (5)$$

where  $\|\cdot\|_F$  denotes the Frobenius norm, and  $\lambda_W$  and  $\lambda_H$  are regularization parameters that balance the trade-off between the fidelity of the approximation and the complexity of the matrices.

NMF is also well suited for dimensionality reduction, particularly in the analysis of FTIR spectroscopy data, where the high-dimensional spectral data necessitate efficient methods for uncovering the underlying biochemical compositions. By decomposing the high-dimensional FTIR spectra matrix  $V$  into two lower-dimensional matrices,  $W$  and  $H$ , NMF retains the essential spectral features while significantly reducing the dataset’s complexity. The matrix  $W$  captures the reduced-dimensional basis spectra representing distinct biochemical components, and  $H$  encodes the corresponding abundances of these components across the samples. This dimensionality reduction facilitates the identification of latent structures within the data, enhancing interpretability and computational efficiency.

## 2.2 Gaussian Mixture Model (GMM)

The Gaussian Mixture Model (GMM) is a probabilistic model for soft classification, which can be effectively applied to the classification of kidney stones due to their composite nature. GMM represents data as a combination of several Gaussian distributions, each corresponding to a different class within the dataset. This approach is highly relevant for kidney stone analysis, where stones may consist of various components like calcium oxalate, uric acid, struvite, cystine and others. Unlike hard classification methods, GMM assigns to each sample a probability of belonging to various classes, acknowledging that kidney stones can contain a mixture of chemical compounds.

A GMM is defined by the equation:

$$p(x) = \sum_{k=1}^K \pi_k \mathcal{N}(x|\mu_k, \Sigma_k) \quad (6)$$

where  $p(x)$  represents the probability of observing a data point  $x$  within the mixture model,  $\pi_k$  are the mixing coefficients indicating the weight of each Gaussian component in the mixture,  $\mu_k$  and  $\sigma_k$  are the mean and covariance of the  $k$ -th Gaussian component, respectively, and  $K$  denotes the number of components in the model. The Gaussian density function for each component is expressed as:

$$\mathcal{N}(x|\mu_k, \Sigma_k) = \frac{1}{(2\pi)^{d/2} |\Sigma_k|^{1/2}} \exp\left(-\frac{1}{2}(x - \mu_k)^T \Sigma_k^{-1} (x - \mu_k)\right) \quad (7)$$

with  $d$  representing the dimensionality of the data. To estimate the parameters ( $\mu_k$ ,  $\Sigma_k$  and  $\pi_k$ ) of the GMM the Expectation-Maximisation (EM) algorithm is employed, which iteratively performs two steps until convergence. The E-step calculates  $\gamma(z_{nk})$ - the probability that data point  $x_n$  belongs to the  $k$ -th Gaussian component, as follows:

$$\gamma(z_{nk}) = \frac{\pi_k \mathcal{N}(x_n|\mu_k, \Sigma_k)}{\sum_{j=1}^K \pi_j \mathcal{N}(x_n|\mu_j, \Sigma_j)} \quad (8)$$

where  $\mathcal{N}(x_n|\mu_k, \Sigma_k)$  denotes the probability density function of the Gaussian distribution for the  $k$ -th component evaluated at point  $x_n$ . The parameters  $\mu_k$ ,  $\Sigma_k$ , and  $\pi_k$  are the mean, covariance, and mixing coefficient of the  $k$ -th component, respectively, and  $K$  is the total number of Gaussian components in the mixture.

Subsequently, the M-step updates the parameters in the following way:

$$\mu_k^{new} = \frac{1}{N_k} \sum_{n=1}^N \gamma(z_{nk}) x_n \quad (9)$$

$$\Sigma_k^{new} = \frac{1}{N_k} \sum_{n=1}^N \gamma(z_{nk}) (x_n - \mu_k^{new})(x_n - \mu_k^{new})^T \quad (10)$$

$$\pi_k^{new} = \frac{N_k}{N} \quad (11)$$

with  $N_k$  being the effective number of data points assigned to component  $k$ .

Each Gaussian component in the mixture model is defined by its mean, which represents the average spectral features of a stone type, and covariance, which accounts for the variability and relationships between features. The soft classification provided by GMM reflects the complex reality of kidney stone compositions, allowing for overlapping classifications. Parameter estimation in GMM uses the Expectation-Maximization (EM) algorithm, which alternates between assigning data points a probability of class membership (expectation step) and updating the model parameters to maximize the data's likelihood given these probabilities (maximization step). This model's ability to handle data complexity and provide probabilistic class memberships makes it suitable for kidney stone classification from FTIR spectral data.

### 2.3 Comparing Spectra Using Euclidean Distance

Prior to the application of the Euclidean distance measure, an additional processing step is undertaken to align the data points across the spectra. Given the inherent variability in the spectral data acquisition process, the spectra of base components and those of patient-derived kidney stones may not have data points recorded at identical wavenumbers. To address this issue, we use one-dimensional linear interpolation where necessary to align the kidney stones' spectra to the spectra of reference materials, utilizing 1-spline techniques for precise alignment.

To ensure consistency in our comparisons, data points from the base spectra were chosen. Any missing data points in the kidney stones' spectra were filled in through interpolation. Following this, the Euclidean distance between each patient stone's spectrum and the spectra of the base materials is computed. The base component spectrum that is closest to the patient stone's spectrum, determined by the minimum Euclidean distance, is chosen as the component of the kidney stone.

## 2.4 NMF-GMM Method of the Identification of Kidney Stone's Composition

In order to decompose kidney stone's FTIR spectrum into individual components we use the combination of NMF and GMM methods. First, we decompose each spectrum into 100 non-negative components using NMF. Then GMM model was fitted using  $K = 14$  Gaussian components in the mixture, one for each base material available in the dataset. After that, the predictions of kidney stones' composition were made using 100 features obtained after NMF decomposition.

## 2.5 Concordance Metric

In our analysis, concordance is defined as the almost exact match between the AI algorithm's predictions and the kidney stone classifications detailed in the urologist's report. Recognizing that urologists manually interpret spectral plots, a certain degree of variability in their initial kidney stone type assignments is inevitable, due to the subjective nature of manual analysis. Consequently, laboratory standards permit a degree of fluctuation in the component composition percentages ( $\pm 20\%$ ), under the condition that the algorithm accurately identifies all components present in the kidney stones.

Accordingly, our concordance metric deems a prediction 'correct' if it accurately identifies the components as reported by the urologist, allowing for a compositional variance of up to 20%. For instance, a kidney stone comprised solely of calcium oxalate dihydrate would necessitate a prediction of this component alone for accuracy; the presence of any additional components would render the prediction incorrect. In cases where the stone is composed of multiple components, with one constituting 90% calcium oxalate dihydrate, predictions are considered correct if they estimate calcium oxalate dihydrate to comprise between 70% and 100% of the stone, provided that any secondary components are also precisely identified within the  $\pm 20\%$  compositional range. This metric serves to evaluate the algorithm's effectiveness in both identifying the presence of specific kidney stone components and estimating their proportions within the stone.

## 3 Data

The internal dataset from Vilnius University Hospital Santaros Clinics was used, focusing on the analysis of seven fundamental components commonly found in kidney stones. These components include albumin, calcium oxalate dihydrate, calcium oxalate hydrate, calcium phosphate dibasic dihydrate, calcium phosphate dibasic, hydroxyapatite, and uric acid crystalline. The spectral plots corresponding to each of these components are illustrated in Fig. 1, providing a visual representation of their characteristic absorption patterns. In addition to these spectra of the base components, FTIR spectroscopy data of 91 kidney stone was analysed. The kidney stones were obtained from patients before FTIR analysis

**Table 1.** Frequency of base components of single-component kidney stones

Component	Frequency
Calcium Oxalate Hydrate	31
Uric Acid Crystalline	25
Calcium Oxalate Dihydrate Rock	5
Calcium Phosphate Dibasic Dihydrate	2
Calcium Phosphate Dibasic	2

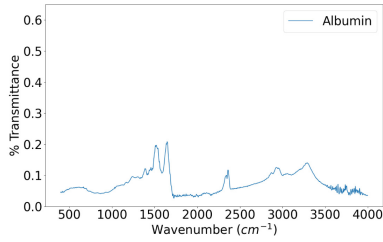
**Table 2.** Frequency of most prevalent component of multi-component kidney stones.

Component	Frequency
Uric Acid Crystalline	5
Calcium Oxalate Hydrate	4
Calcium Oxalate Dihydrate Rock	4
Albumin	1

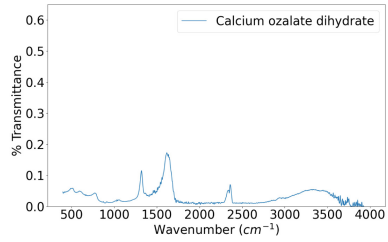
**Table 3.** Frequency of second most prevalent component of multi-component kidney stones.

Component	Frequency
Hydroxyapatite	3
Calcium Oxalate Hydrate	3
Calcium Phosphate Dibasic	3
Albumin	2
Uric Acid Crystalline	1
Calcium Phosphate Dibasic Dihydrate	1
Calcium Oxalate Dihydrate Rock	1

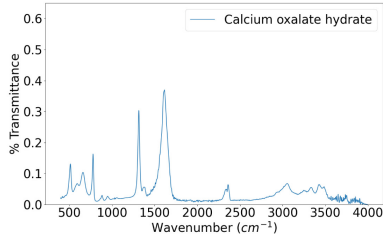
was conducted. 77 of these patients had single-component kidney stone samples, where the most frequent component was calcium oxalate hydrate, as shown in Table 1, which is consistent with previously discussed studies. 14 patients had multi-component kidney stones. The frequency of most prevalent component and secondary component in the dataset is shown in Tables 2 and 3 accordingly (Figs. 3, 4, 5 and 6).



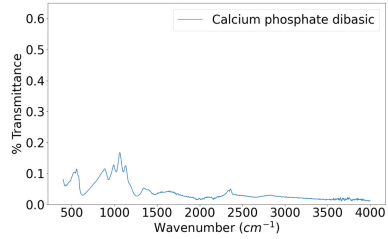
(a) Albumin



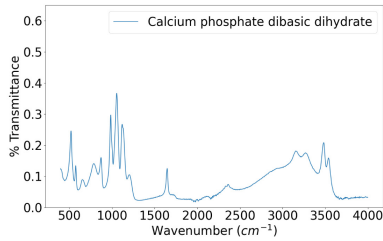
(b) Calcium Oxalate dihydrate



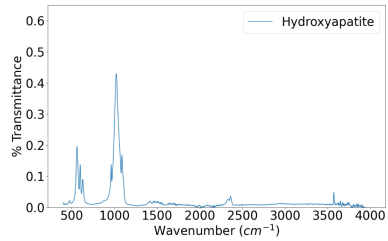
(c) Calcium oxalate hydrate



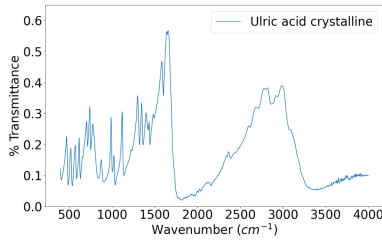
(d) Calcium phosphate dibasic



(e) Calcium phosphate dibasic dihydrate

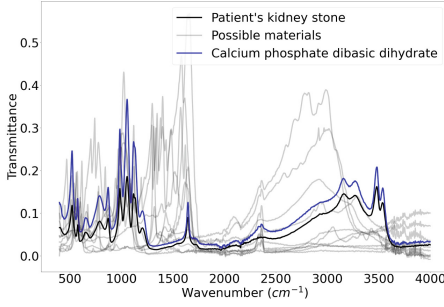


(f) Hydroxyapatite

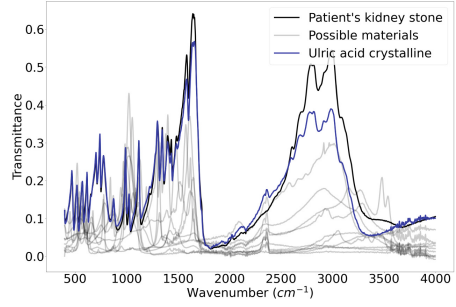


(g) Uric acid crystalline

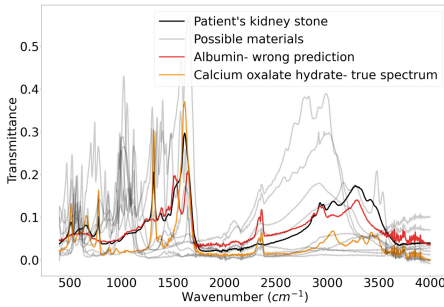
**Fig. 1.** Spectra of kidney stones' components.



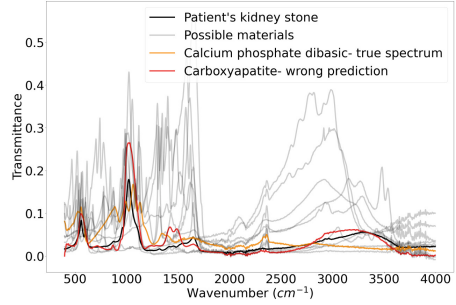
(a) Correct prediction of calcium phosphate dibasic dihydrate.



(b) Correct prediction of ulric acid crystalline.



(c) Misidentified calcium oxalate hydrate.



(d) Misidentified calcium phosphate dibasic.

**Fig. 2.** Examples of predictions of kidney stone components using NMF and GMM.

## 4 Results

We begin by evaluating the baseline performance through a simple method for comparison, utilising Euclidean distance for spectra comparison. This serves as a foundation for assessing the effectiveness of NMF-based methods. Following this, we explore the outcomes of applying NMF alone and investigate its capability for dimensionality reduction using the combined approach, where NMF serves as a preliminary step for dimensionality reduction, followed by the application of the GMM for soft classification.

### 4.1 Euclidean Distance Based Spectra Comparison

Table 4 presents the concordance percentage and F1 score achieved through the Euclidean distance-based method, revealing relatively low performance metrics with a concordance percentage of 40% and an F1 score of 0.3. The under-performance can be attributed to the method's limitations, particularly how significant discrepancies in major spectral peaks disproportionately influence the Euclidean distance calculation, leading to incorrect classification of kidney

stones. This occurs despite the possibility of minimal mismatches across other spectral regions.

## 4.2 NMF for Spectral Analysis

Employing NMF alone improves the results, with a concordance percentage of 75% and F1 score of 0.732 (see Table 4). NMF proves to be more effective for comparing spectra, as it employs a factorisation approach that decomposes the spectra into a basis set and coefficients, reflecting the underlying structure of the data. This decomposition method is particularly advantageous because it isolates significant patterns within the spectra, facilitating a more nuanced comparison that is less affected by variations in magnitude or isolated discrepancies in the spectral data.

## 4.3 Applying NMF for Dimensionality Reduction in Combination with Other Machine Learning Techniques

NMF was also applied as a method for dimensionality reduction in conjunction with GMM for classification purposes. By utilising NMF, we reduced the feature space to 20 and 100 significant features, which were then used for classifying each spectrum. The results show a concordance percentage of 75% and an F1 score of 0.875 (Table 4). The improvement in the F1 score indicates a higher accuracy in identifying the correct components of kidney stones within the test set. However, the concordance percentage remained unchanged, suggesting that while more components were correctly identified, their quantified percentages were often inaccurate. Introducing a more diverse dataset, particularly with a broader range of component concentrations in multi-component stones, could potentially improve these results further.

Additional machine learning methods were also explored, together with a different number of features retained after dimensionality reduction using NMF. While some of these methods achieved higher F1 scores compared to the combination of NMF and GMM - indicating a greater accuracy in identifying kidney stone components - the concordance percentages were notably lower. This lower concordance suggests that, despite correctly identifying more components, the estimated proportions of these components were often incorrect.

Figure 2 presents examples of kidney stones' spectra alongside their predictive analyses. Plots Fig. 2a and 2b illustrate instances where components have been accurately identified, whereas plots Fig. 2c and 2d display cases of misidentification. Intriguingly, to those not specialized in the field, the erroneous predictions in plots Fig. 2c and 2d may seem more closely aligned with the spectra of the correct components.

**Table 4.** The results of kidney stones composition analysis.

Method	Concordance percentage	F1 score
Euclidean distances predictor	42.27%	0.375
NMF 100 features + Gaussian Mixture Model	75.00%	0.875
NMF only	75.00%	0.732
NMF 100 features + Logistic Regression	18.75%	0.875
NMF 100 features + SVR	18.75%	0.728
NMF 20 features + Random Forest Classifier	59.09%	0.807
NMF 100 features + Random Forest Classifier	18.75%	0.838
NMF 20 features + LGBM	59.09%	0.786
NMF 20 features + XGB	68.18%	0.786
NMF 20 features + MLP	18.18%	0.760
NMF 100 features + MLP	68.75%	0.931

## 5 Conclusions

In our investigation, the composition of kidney stones' spectra was analysed using NMF alongside various machine learning models. Using NMF significantly enhanced the analysis when compared to basic Euclidean distance comparisons. This improvement can be attributed to NMF's ability to decompose complex spectra into a set of meaningful components, revealing intrinsic patterns that simple distance metrics cannot capture. Such a decomposition not only aids in distinguishing between different types of kidney stones, but also in identifying subtle variations within the spectra that are characteristic of specific components.

An important finding from our analysis is the realization that a high F1 score, which is typically a desirable metric in classification tasks, does not fully encapsulate the clinical relevance of the predictions. In the context of kidney stone analysis, the ability to accurately quantify the composition of kidney stones - identifying not just the presence of certain components but also their proportions - is paramount. This aspect is crucial for clinical practice, where treatment decisions may depend on the precise makeup of the stone rather than merely its constituent components.

Moving forward, creating a more diverse dataset, especially with varied multi-component stones, is crucial for improving the precision of component percentages, enhancing the analysis's clinical relevance. Additionally, the accuracy of data labels needs rigorous review, as illustrated by the mispredictions in Fig. 2, where predicted spectra occasionally matched actual samples better than the true components. This highlights the importance of validating label collection methods for more reliable analysis.

The challenges faced in accurately quantifying kidney stone components underscore the complexity of analyzing spectral data for clinical use. Enhancing

dataset diversity and label accuracy could improve outcomes to be more clinically relevant. Further refining NMF and machine learning techniques, perhaps by incorporating specialized knowledge or advanced models, may lead to more precise analyses. The ultimate aim is to develop methods that reliably guide treatment, thus bettering patient care in kidney stone management.

**Disclosure of Interests.** The authors have no competing interests to declare that are relevant to the content of this article.

## References

1. Tsujihata, M.: Mechanism of calcium oxalate renal stone formation and renal tubular cell injury. *Int. J. Urol.* **15**(2), 115–120 (2008)
2. Ivanovski, O., Drüeke, T.B.: A new era in the treatment of calcium oxalate stones? *Kidney Int.* **83**(6), 998–1000 (2013)
3. Pearle, M.S., et al.: Medical management of kidney stones: AUA guideline. *J. Urol.* **192**(2), 316–324 (2014)
4. Zisman, A.L.: Effectiveness of treatment modalities on kidney stone recurrence. *Clin. J. Am. Soc. Nephrol. CJASN* **12**(10), 1699 (2017)
5. Moe, O.W.: Kidney stones: pathophysiology and medical management. *Lancet* **367**(9507), 333–344 (2006)
6. Servais, A., et al.: Cystinuria: clinical practice recommendation. *Kidney Int.* **99**(1), 48–58 (2021)
7. Kotaska, K., Werle, J., Hosnedlova, B., Kizek, R., Prusa, R.: Use of Fourier transform infrared (FTIR) spectroscopy to detect rarely occurring cyanoacrylate and pyrophosphate urine stones. *Appl. Spectrosc. Rev.* **58**(10), 724–737 (2023)
8. Sofińska-Chmiel, W., et al.: Chemical studies of multicomponent kidney stones using the modern advanced research methods. *Molecules* **28**(16), 6089 (2023)
9. Steenbeke, M., De Buyzere, M.L., Speeckaert, M.M., Delanghe, J.R.: On the protein content of kidney stones: an explorative study. *Acta Clinica Belgica* **77**(5), 845–852 (2022)
10. Gilad, R., et al.: Interpreting the results of chemical stone analysis in the era of modern stone analysis techniques. *J. Nephrol.* **30**, 135–140 (2017)
11. Day, P.L., et al.: Artificial intelligence for kidney stone spectra analysis: using artificial intelligence algorithms for quality assurance in the clinical laboratory. *Mayo Clin. Proc. Digit. Health* **1**(1), 1–12 (2023)
12. Singh, V.K., Jaswal, B.S., Sharma, J., Rai, P.K.: Analysis of stones formed in the human gall bladder and kidney using advanced spectroscopic techniques. *Biophys. Rev.* **12**(3), 647–668 (2020). <https://doi.org/10.1007/s12551-020-00697-2>